The paper is organized as follows. Section II summarizes several related works with applications in monitoring of cargo containers. Section III presents an overview of the whole system. Ultrasonic channel characterization is detailed in Section IV. From the obtained results, an enhanced ultrasonic front-end topology is proposed in Section V. Section VI describes the experimental results and Section VII presents a comparative study of similar research works. Finally, conclusions are drawn in Section VIII.

II. Related Works

The main concepts and benefits of automatizing the containers terminals were originally evaluated in [13]. By using the basis explored in [13], more recent research works have studied how to optimize the logistics algorithms to improve location, tracking and planning for roads [12], trains [14] and specially container seaports [15]-[16] applications. This interest is due to the fact that these maritime terminals represent the main interface and iteration point between the different freight transportation modalities. However, all these approaches do not provide an integrated solution with monitoring of goods functionalities. Besides, there are several complete solutions at research [17] and commercial [18] levels. However, these solutions present some drawbacks, such as using wireless communication at 2.4 GHz (leading to communication issues due to the high density of stacked metal containers) and the use of invasive solutions, which need to drill the container surface to collect the sensed variables.

In order to overcome these limitations, [6] proposed, respectively, the use of both a low power wireless network at 868/915 MHz and ultrasonic communication through the container metallic walls. This solution was selected over other non-invasive technologies, such as RFID, which presents collision and electromagnetic propagation problems for harsh scenarios with many stacked containers, and also reduced efficiency for monitoring and location purposes [19]. Other discarded non-invasive solutions are based on Optical Character Recognition (OCR) [20] and computer vision-based techniques [21]. These techniques imply more complex and error-prone processes, due to the high dependence with the properties of the container surface, which can be deteriorated during the transport, and also with conditions such as angle of view, distance or luminosity.

Finally, a numerical comparison between other related works based on ultrasonic communication through metal barriers, for low data rate [1]-[3], [6] and high data rate applications [4]-[5], will be detailed in Section V. More specifically, as mentioned above this paper presents an enhanced version of the previous work [6], focused on overcoming some limitations regarding power consumption, robustness and signal bandwidth. The main novelties of the proposed system regarding [6] can be summarized as follows:

a) Power consumption is reduced considerably by using a new transducer-metal coupling method more robust against fluctuations and with higher signal bandwidth and sensitivity, allowing reduction of the voltage generated at the input of the ultrasonic transducer at the transmitter side.

b) The proposed transmitter implementation exploits the non-linearity of the metallic channel, by transmitting a 5th harmonic over the operation frequency of the ultrasonic transducer. This innovative solution reduces the power consumption in the transmitter, which is a critical requirement for devices installed inside the container.

c) Power consumption is also reduced in the receiver side by implementing a subsampling based process for non-linear scenarios, which allows the use of low-cost electronics for higher data rates. Also, the employed carrier and sampling frequencies have been properly selected in order to avoid the use of a Direct Digital Synthesizer (DDS), reducing the complexity at the transmitter and receiver sides.

d) A more reliable modulation scheme (128-OFDM instead of DBPSK) is proposed in order to exploit the observed higher signal bandwidth. This multi-carrier modulation reduces the transmission times, improves robustness against fading effects and fluctuations of carrier frequency, and increases the spectrum efficiency. This latter advantage would allow higher data rates, extending the sensor capabilities. For example, by increasing the number of measurements, or including high data rate information.

III. System Overview

The proposed overall system is composed of:

- Sensors inside the container.
- Ultrasonic communication link to extract information from the sensor handler to the transponder controller, both based on low power microprocessors.
- A wireless network to transmit the information between the containers.
- The internet-gateway and dedicated software to manage the information. This information will be presented to the final user and it will be used for tracking and monitoring purposes.

The features and functionalities of each part were detailed in [6] and can be identified in Figure 1. The system, based on non-invasive communication and portable devices, has a reduced cost-factor of design, manufacturing and maintenance, having a scalable price of 200-300€ per container, almost irrelevant compared with the investment for a container and the associated shipment costs.

The system was designed to work properly on a harsh environment based on stacked metallic containers, by selecting the frequency band 868/915 MHz (IEEE 802.15.4 standard), with worldwide compatibility, high information bandwidth and oriented to low power and efficient sensor networks. The proposed solution optimizes signal bandwidth and power consumption, by redesigning the ultrasonic communication link, as will be described in the next sections.

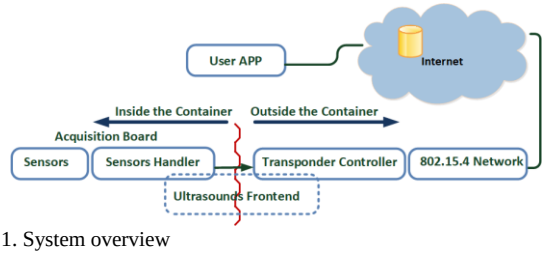

Figure 1. System overview

IV. Ultrasonic Channel Description

A. Ultrasonic Technology Selection

Piezoelectric transducers have been selected over other technologies, such as laser and electromagnetic acoustic transducers (EMAT), due to their higher maturity, transducers size, power efficiency, lower maintenance costs and higher data rates [22]. The main drawback associated to the piezoelectric techniques is the induced multipath propagation, leading to Inter-Symbol Interference (ISI). This limitation will be minimized, using a multi-carrier OFDM modulation, by selecting a proper cyclic prefix, as described in Section V. This allows increasing the carrier frequency and exploiting the benefits of these modulations regarding spectrum efficiency. The employed piezoelectric transducer is the model Prowave 400EP250 model, with a carrier frequency at 40 KHz.

B. Transducer-Metal Coupling Selection

The performance of the ultrasonic channel depends to a large extent on the quality of the coupling between the metallic wall and the ultrasonic transducer. In the previous system proposed in [6], a magnetic enclosure was employed to attach the transducers to the container wall, allowing an easy and versatile installation. However, this type of coupling can reduce the stability of the channel with respect to the frequency response, due to a lower acoustic impedance matching caused by insufficient pressure or surface roughness.

Other coupling methods based on permanent adhesives have been widely used in the literature [3], providing higher physical resistance and improved stability of the ultrasonic channel, at the expense of a more tedious installation.

In this context, both coupling approaches, i.e., the magnetic enclosures employed in [6] and the fixation using an adhesive (Araldite 2011 Epoxy), have been experimentally compared. A painted steel plate with an area of 1 m^2 and a thickness of 0.7 cm has been employed for emulating the properties of the real cargo container in this preliminary test, placing the aligned transducers at both sides of the plate.

The main conclusion was the strong dependence of the frequency response with the coupling method used. The experimental results are shown in Figure 2. As can be observed, the transducers fixed with epoxy clearly offer a higher sensitivity, except for a narrow band around the nominal operating frequency (40 KHz), where the system using magnetic cases presents its higher resonance peak. Moreover, it has been verified that the magnitude of this peak presents a slight variation (between 40-45 KHz) for different experiments. This drift is due to a reduction of acoustic impedance matching. In contrast, the transducers attached with epoxy offer a higher stability in a wide bandwidth, especially at higher frequencies, being the maximum sensitivity at around 360 KHz.

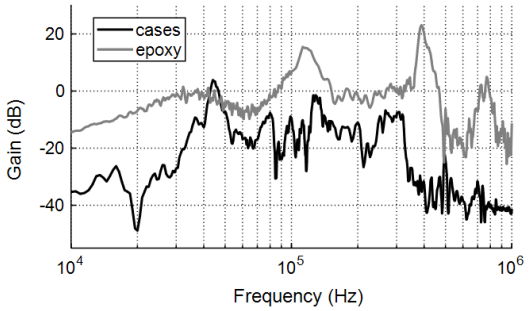

Figure 2. Frequency response using epoxy and magnetic cases

Additionally, note that the maximum of the transmitted ultrasonic wave is located at [2]:

$$N = \left(D^2 - \lambda^2\right)/4\lambda \quad (1)$$

where D is the diameter of the transducer (25 mm) and $\lambda = v/f$ is the wavelength, with the acoustic propagation velocity $v \approx 5150$ m/s for steel and $f = 360$ KHz. Thus, N results 0.735 cm, very similar to the metallic barrier thickness (0.7 cm), so the transmitter will work close to the optimal case. Therefore, the solution adopted to implement the final system will be based on epoxy coupling methods, instead of the magnetic cases used in [6], in order to exploit some features such as:

- A minimal frequency variation.
- High gain, up to 20 dB higher than working at the nominal resonance frequency using magnetic cases.
- Higher signal bandwidth (around 30 KHz) than working at the nominal resonance frequency (10 KHz) [6].

Although using low frequencies has some benefits regarding insertion losses and robustness against multi-path effects, the advantages found by transmitting around the 360 KHz band will lead to improve the overall performance of the communication system, as described in Section V.

V. Communication System Based on OFDM

A. Modulation parameters and employed devices

An OFDM modulation is implemented in order to exploit the higher bandwidth observed in the channel and provide additional robustness to the communication link. The implemented OFDM modulation is a simplified version of the standard PRIME v1.3.6 (PoweR line Intelligent Metering Evolution, standard developed by Power Line Communication).

. The main modulation parameters are the following:

- 128 carriers (97 active carriers).
- Possible modulations: DBPSK, DQPSK and D8PSK.
- Optional convolutional FEC.
- Cyclic prefix of 16 samples.
- Preamble for detection and synchronization purposes based on a chirp of 40 samples.
- Signal bandwidth of 24.5 kHz.
- Separation between the carriers of 250 Hz.

In order to reduce the power consumption, modulation and demodulation processes are implemented by software using two

low-cost microcontrollers 32bit-ARM Cortex-M3 STM32F103RD. With the same objective, the 12-bit DAC and ADC embedded in the microcontroller have been employed.

B. Transmitter implementation

A diagram of the implemented OFDM system is shown in Figure 3.The transmitter (TX) encodes a binary data stream to generate discrete-time OFDM symbols, using a convolutional FEC (Forward Error Correction) with code generator polynomials equal to 1111001 and 1011011. This FEC can be disabled in order to increase the overall bitrate. After coding, the binary stream is randomized by the scrambler block, reducing the crest factor when there is a long stream of '0's or '1's. Due to frequency fading, OFDM subcarriers are usually received with different amplitudes and, therefore, some groups of subcarriers can be less reliable than others, causing more bit errors in bursts if they are not randomly scattered. Moreover, the interleaver permutes the order of bits to ensure that originally adjacent bits are separated by several bits.

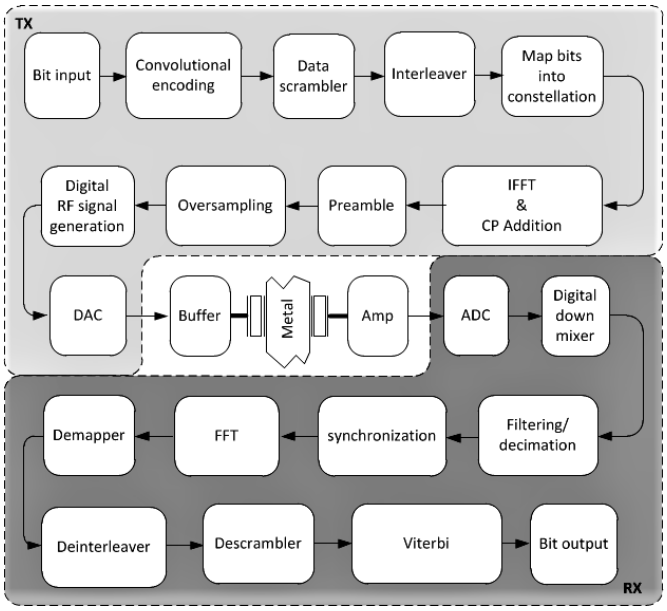

Figure 3. Block diagram of the OFDM system

After the interleaving process, the binary data is modulated as a multi-carrier DPSK signal with a pilot and 128 data subcarriers allowing the transmission of 128, 256 or 512 bits per symbol. The frequency domain OFDM symbol is converted to time domain by means of an IFFT process and the cyclic prefix is added to cancel the multipath effect. In order to carry out the synchronization process at the receiver side, a preamble is added at the beginning of the transmission frame. After that, the signal is up-converted to 72 KHz and then converted to the analog domain by using a 12-bit DAC.

This carrier frequency (f_{c1}) of 72 KHz has been selected with the objective to generate the signal directly, without using an external quadrature mixer, thus reducing costs. Thus, we select a DAC sampling frequency (fs_1) of 288 KHz, i.e., $f_{s1}=4 \bullet f_{c1}$. This frequency plan allows the immediate implementation of a digital mixer, without implementing a DDS, i.e., only using values of ±1 and 0 for the mixing process. Moreover, by selecting this value of f_{c1}, it is possible to exploit the high non-linearity of the channel to transmit a signal located at 360 KHz, using the 5th harmonic of the generated signal. This solution allows to transmit within the band of highest gain for the case of epoxy attachment (Figure 2), maintaining the use of a low cost DAC embedded in the microcontroller. Finally, a buffer is employed to drive the ultrasonic transducer.

C. Receiver implementation

1) Charge amplifier stage

This stage performs the charge-voltage conversion of the ultrasonic signal, as was described in [6], and it is based on an operational amplifier (OPA350 of Texas Instruments) with a negative feedback loop composed by a capacitor (C_f) and a resistor (R_f), leading to a 1st-order high pass response, with a cutoff frequency at $1/(2\pi C_f R_f)$ and a sensitivity inversely proportional to C_f. A value of 10 pF for C_f and a R_f higher than 50 KΩ have been selected in order to maximize the sensitivity and to place the band of interest (i.e., a signal centered at 360 KHz with 24.5 KHz of signal bandwidth) in the pass-band of the amplifier.

2) Analog-to-digital conversion stage

For this application we propose to implement a subsampling based receiver, in order to reduce the power consumption at the external node and to implement a detection process portable to lower cost ADCs. For a bandpass signal centered at f_c with a signal bandwidth B, the subsampling frequency (f_s) has to meet Equation 2 [23], in order to avoid aliasing between the replicas folded in the spectrum:

$$2(f_c - B/2)/(m-1) > f_s > 2(f_c + B/2)/m \qquad (2)$$

where m is the number of replicas of the signal in the range [0, $f_c - B/2$], with a value between 1 and $floor((fc + B/2)/B)$. Additionally, for a nonlinear environment, as the described ultrasonic metal channel, there are additional challenges to avoid aliasing between the different harmonics. For these scenarios, the selected sampling frequency has to meet this additional requirement [24]:

$$if_c + n_k f_s \le jf_c < if_c + (n_k + 1) f_s \qquad (3)$$

where if_c and jf_c are two harmonics of f_c and $n_k = floor\ ((jf_c - if_c)/f_s)$. Since this implementation is a particular case, working with the 5th harmonic as signal of interest (f_c), we assign to i and j values multiples of 1/5 instead of integer values, avoiding aliasing between the 5th harmonic and the original signal at 72 KHz and its 2nd-4th and 6th harmonics. A 6th order non-linearity has been assumed since the channel response attenuates around 40 dB the >6th order harmonics, as shown in Figure 2.

Between the valid sampling ranges given by (2)-(3), sampling frequency (f_{s2}) of 320 KHz is selected, so that f_{c1} (at 360 KHz) is folded to 40 KHz (f_{c2}). Therefore, the digital mixing process is implemented by ADC sampling, reducing the used resources. Since the sampling frequency is $f_{s2}=8 \bullet f_{c2}$, it is not necessary to use a DDS, due the samples of the discrete sine and cosine only require the values of ±1, ±1/√2 and 0.

3) Digital domain stage

In the digital domain the signal is down-converted, filtered and decimated, as illustrated in Figure 3, in order to obtain the baseband complex OFDM symbols. Time synchronization is carried out using a simple correlation with the received signal and the preamble. Next, the cyclic prefix, which can be corrupted by the multipath echoing, is removed. Each time-

domain OFDM symbol is processed by the FFT block, recovering the magnitude and phase of each OFDM subcarrier. Then, the data carriers are demapped, deinterleaved and descrambled, and finally decoded using a Viterbi decoder.

VI. Experimental Results

For this test, the transducers were fixed to the metallic wall, faced at both sides of the cargo container (with a thickness of 7 mm and dimensions according to the International Standards Organization (ISO) [19]), as illustrated in Figure 4.

With the objective to decide the optimal modulation in terms of BER and energy efficiency, a comparison between three modulations, with five different voltage levels at the DAC output, and with or without using a FEC, is presented. For each experimental measurement, 2000 data bursts, with length of 33 bytes, are transmitted. The results are shown in Table I, where it is possible to observe the expected performance, i.e., a higher robustness when a FEC and a higher input voltage are employed. However, even for a minimal input voltage, the obtained BER results satisfactory.

Figure 4. Transponder controller outside the container (left) and acquisition board inside the container (right)

Additionally, the energy consumption has been evaluated for the same 30 scenarios. These results are presented in Table II, showing the energy consumed by data burst (33 bytes), assuming a normalized resistance of 1 Ω. The transmission time can be expressed as:

$$T_{tx} = (N_{pr} + (N_{cp} + N_{ifft})N_{sym}) / f_{bb} \qquad (4)$$

where N_{pr}, N_{cp}, N_{ifft} are, respectively, the number of samples per preamble (40), per cyclic prefix (16) and per symbol (128), N_{sym} the number of symbols necessary to transmit 33 bytes for each modulation, and f_{bb} the baseband sampling frequency (32 KHz).

TABLE I
Bit Error Rate for the different scenarios

	50 mV_{rms}	25 mV_{rms}	12 mV_{rms}	7 mV_{rms}	4 mV_{rms}
DBPSK	0[1]	0	0	0	0.00007
DQPSK	0	0	0	0.00024	0.0149
D8PSK	0	0.0003	0.003	0.02040	0.0718
DBPSK+FEC	0	0	0	0	0
DQPSK+FEC	0	0	0	0	0
D8PSK+FEC	0	0	0	0.00039	0.00079

[1] 'BER=0' strictly equals to BER < $2 \cdot 10^{-5}$ (in order to implement more reliable measurements, the error condition is given by receiving at least 10 wrong bits, i.e., the resolution is 10 errors/(2000 data bursts • 33 bytes • 8 bits)).

TABLE II
Normalized energy consumption [μJ] for the different scenarios

	50 mV_{rms}	25 mV_{rms}	12 mV_{rms}	7 mV_{rms}	4 mV_{rms}
DBPSK	36.875	9.21875	2.124	0.72275	0.236
DQPSK	25.625	6.40625	1.476	0.50225	0.164
D8PSK	14.375	3.59375	0.828	0.28175	0.092
DBPSK+FEC	70.625	17.65625	4.068	1.38425	0.452
DQPSK+FEC	36.875	9.21875	2.124	0.72275	0.236
D8PSK+FEC	25.625	6.40625	1.476	0.50.225	0.164

Moreover, EVM (Error Vector Magnitude) has been calculated and is shown in Table III. This figure of merit, which is independent of modulation, measures how far the constellation points are from the ideal locations, and is mathematically given by (5) [25]:

$$EVM = \frac{\sum_{i=1}^{L}\sum_{k=2}^{65}\left|r_k^i - r_{k-1}^i e^{-(j2\pi/M)\Delta b_{k-1}}\right|^2}{\sum_{i=1}^{L}\sum_{k=2}^{65}\left|r_k^i\right|^2} \qquad (5)$$

where L is the number of OFDM symbols, r_k^i denotes the k^{th} carrier of the FFT output for symbol i. Δb_k represents the decision on the received information symbol coded in phase increment, and M is the number of constellation symbols, i.e., 2, 4, or 8 for DBPSK, DQPSK or D8PSK, respectively.

TABLE III
EVM for the different scenarios

	50 mV_{rms}	25 mV_{rms}	12 mV_{rms}	7 mV_{rms}	4 mV_{rms}
DBPSK	19.8	18.86	16.51	12.56	7.78
DQPSK	19.24	18.63	16.12	12.25	7.49
D8PSK	19.42	18.68	16.14	12.29	8.83
DBPSK+FEC	19.16	18.38	16.24	12.3	7.64
DQPSK+FEC	18.95	18.29	16.27	12.31	7.82
D8PSK+FEC	19,15	18.5	16.24	12.42	8.78

From this analysis, it is possible to observe how the optimal modulation in terms of accuracy results on a D8PSK (at 50 mV_{rms}), since it minimizes the consumed energy between scenarios with minimum BER and maximum EVM. For cases where the energy consumption is the main requirement, the best option correspond to a DQPSK with the activated FEC (at 4 mV_{rms}), considering the scenarios with minimal BER.

Figure 5 (left) illustrates the constellation measured for a D8PSK, where it is possible to observe how the locations between the eight regions are sufficiently separated. Figure 5 (right) shows the 256 points-FFT of the channel response. It is possible to observe how, for the band of interest (59.75-84.25 KHz), is very close to the maximum gain region, with a gain ripple of 58 points, i.e., 1.16 dB.

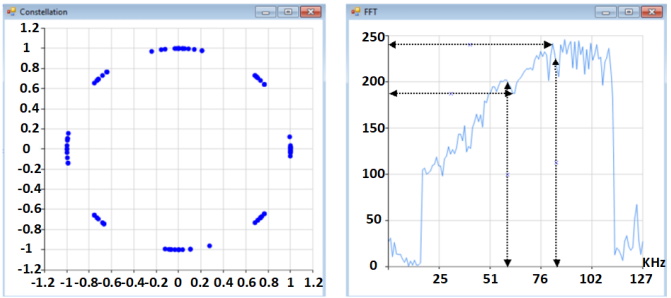

Figure 5. Constellation (left) and channel response (right) for a D8PSK

VII. Comparative Analysis

A comparative study of ultrasonic systems through metal walls is shown in Table IV, which includes the features of the proposed system and the previous version presented in [6].

In this table, only [4] uses EMAT instead of piezoelectric technologies, presenting a lower power efficiency, typical of EMAT technologies. Additionally, although [4]-[5] provides a high data rate performance, they also present higher power consumption since the attenuation through the metal channel increases with the frequency. This higher power consumption is also due to they use thicker metallic barriers, as the case presented in [1]. For low power applications, such as [2]-[3], the proposed system considerably improves the power consumption and the data rate, by using an OFDM instead of an AM modulation, leading to enhanced features regarding transmission times and spectrum efficiency.

Furthermore, it is possible to observe how the proposed system significantly improves the previous version [6]. Firstly, by using the resonance band at 360 KHz, it is possible to increase the signal bandwidth up to 24.5 KHz, which leads to a higher data rate (50.6 Kbps) and a lower transmission time. This time per data burst is minimum (5.75 ms from equation (4)) for the D8PSK case and maximum (28.25 ms) for the DBPSK+FEC, in contrast with the transmission time of 108.8 ms obtained in [6]. Secondly, the proposed system considerably reduces the power consumption (calculated for a 300 Ω-transducer input impedance), by exploiting the gain in the selected band, which is around 20 dB higher than the gain at 40 KHz by using magnetic cases. This power consumption is given for the scenario with higher EVM (input voltage of 50 mV_{rms}), being still possible to reduce this voltage keeping a good performance in terms of BER. Besides exploiting a higher gain, it is possible to reduce this input voltage since the proposed system presents an enhanced robustness against frequency drift and fading effects, by using an epoxy based coupling method and a multi-carrier modulation, respectively.

TABLE IV
Comparison between different related works based on ultrasonic transmission

Publication	Data rate (Kbps)	Modulation	Voltage / Power Input	Bulkhead Thickness (cm)
[1]	0.435	AM	10 V	15.24
[2]	1	AM	30 mW	0.7
[3]	32.5	AM	100 mW	5.7
[4]	1000	QPSK	1230 mW	2.54
[5]	17370	OFDM	31 V	6.35
[6]	2.5	DBPSK	3.3V/36.3 mW	1
This work	50.6	OFDM	141.1 mV/66.7 μW	0.7

This enhanced robustness can also be evidenced by inspecting the reliability of the whole system. Once the performance of the sensors inside the container (i.e., temperature, brightness, humidity, accelerometer, motion and magnetic), the wireless network, the GPS and the server and data browser were validated as described in [6], the integrated system led to a 99.47 % of correct measurements, improving the 97.33% value in [6] for the same number of measurements and three cargo containers monitored simultaneously.

VIII. Conclusions

A low-cost and non-invasive ultrasonic communication based system has been presented for tracking, monitoring and management of cargo containers, where the sealing preservation and the reduction of the power consumption are the main technical challenges. The proposed system employs an OFDM modulation with the objective to increase the data rate and reduce the transmission times. The system uses an epoxy based coupling method in order to improve the robustness against drift of the carrier frequency and to transmit over the nominal frequency of the piezoelectric transducer, increasing the signal bandwidth and the gain at the selected band. As main novelty, we propose to exploit this higher gain and the non-linearity of the channel, transmitting the 5^{th} harmonic of the generated signal, making it possible to reduce the power consumption at the internal node. At the receiver side, a subsampling based system allows to reduce power consumption of the external node. Thanks to the subsampling process, the proposed communication system can be implemented using low-cost and low power electronics. A comparison of different angular modulation has been performed in terms of BER and consumed energy. The designed communication system has been integrated in the whole system, composed of an internal configurable sensor network, a long range and low power scalable wireless IEEE 802.15.4 network at 868/915 MHz, with worldwide compatibility and oriented to harsh scenarios, and a management subsystem for tracking and monitoring purposes. The integrated system has been experimentally validated in a real scenario, leading to a competitive solution for intermodal freight transport, and improving the features of the previous work regarding power consumption, data rate and robustness.

References

[1] G. J. Saulnier *et al.*, "Through-Wall Communication of Low-Rate Digital Data Using Ultrasound," *IEEE Ultrason. Symp.*, pp. 1385-1389, Oct. 2006.

[2] M. Kluge *et al.*, "Remote Acoustic Powering and Data Transmission for Sensors inside of Conductive Envelopes," *IEEE Sensors*, pp. 41-44, Oct. 2008.

[3] J. D. Ashdown, *et al.*, "A Full-Duplex Ultrasonic Though-Wall Communication and Power Delivery System," *IEEE Trans. on Ultrason., Ferroelectr., and Freq. Control*, vol. 60, no. 3, March 2013.

[4] D. J. Graham, J. A. Neasham and B. S. Sharif, "Investigation of Methods for Data Communication and Power Delivery Through Metals," *IEEE Trans. on Ind. Elecron.*, vol. 58, no. 10, pp. 4972-4980, Oct. 2011.

[5] T. J. Lawry *et al.*, "A High-Performance Ultrasonic System for the Simultaneous Transmission of Data and Power Through Solid Metal Barriers," *IEEE Trans. on Ultrason., Ferroelectr., and Freq. Control*, vol. 60, no. 1, pp. 194-205, Jan. 2013.

[6] E. H. Fort *et al.*, "Intelligent Containers Based on a Low-Power Sensor Network and a Non-Invasive Acquisition System for Management and Tracking of Goods," *IEEE Trans. on Intell. Transp. Sys.*, vol. PP, no. 99, pp. 1-6, 2017.

[7] F. Corman *et al.*, "Optimizing Hybrid Operations at Large-Scale Automated Container Terminals," *Models and Technologies for Intelligent Transportation Systems (MT-ITS)*, pp. 514-521, Jun. 2015.

[8] E. Bou-Harb, E. I. Kaisar and M. Austin, "On the Impact of Empirical Attack Models Targeting Marine Transportation," *5th IEEE Intern. Conf. on Models and Technologies for Intell. Transp. Sys. (MT-ITS)*, pp. 200-205, 2017.

[9] G. Cavone, M. Dotoli and C.Seatzu, "A Survey on Petri Net Models for Freight Logistics and Transportation Systems," *IEEE Trans. on Intell. Transp. Syst.*, vol. PP, no. 99, pp. 1-19, 2017.

[10] W. Lang *et al*., "The "Intelligent Container"—A Cognitive Sensor Network for Transport Management," *IEEE Sensors Journal*, vol. 11, no.3, pp. 688-698, Mar. 2011.
[11] R. Jedermann, C. Lloyd and T. Pötsch, "Communication techniques and challenges for wireless food quality monitoring," Philosophical Transactions of the Royal Society A, vol. 372, no. 2017, pp. 1-18, 2017.
[12] A. Abadi, P. A. Ioannou and M. M. Dessouky, "Multimodal Dynamic Freight Load Balancing," *IEEE Trans. on Intell. Transp. Syst.*, vol. 17, no. 2, pp. 356-366, Feb. 2016.
[13] C. I. Liu, H. Jula and P. A. Ioannou, "Design, Simulation, and Evaluation of Automated Containers Terminals," *IEEE Trans. on Intell. Transp. Sys.*, vol. 3, no. 1, pp. 12-26, Mar. 2002.
[14] W. Sun *et al*., "Energy-Efficient Communication-Based Train Control Systems With Packet Delay and Loss," *IEEE Trans. on Intell. Transp. Syst.*, vol. 17, no. 2, pp. 452-468, Feb. 2016.
[15] C. Caballini *et al*., "An Event-Triggered Receding-Horizon Scheme for Planning Rail Operations in Maritime Terminals," *IEEE Trans. on Intell. Transp. Syst.*, vol. 15, no. 1, pp. 365-375, Feb. 2014.
[16] L. Chen *et al*., "Container Port Performance Measurement and Comparison Leveraging Ship GPS Traces and Maritime Open Data," *IEEE Trans. on Intell. Transp. Syst.*, vol. 17, no. 5, pp. 1227-1242, May. 2016.
[17] S. Mahlknecht and S. A. Madani, "On Architecture of Low Power Wireless Sensor Networks for Container Tracking and Monitoring Applications," *5th IEEE Int. Conf. on Ind. Informat.*, vol. 1, no. 1, pp. 353-358, June 2007.
[18] http://www.globetracker.com/gt-sense-genset/
[19] S. Abbate *et al*., "An Integer Linear Programming Approach for Radio-Based Localization of Shipping Containers in the Presence of Incomplete Proximity Information," *IEEE Trans. on Intell. Transp. Syst.*, vol. 13, no. 3, pp. 1404-1419, Sep. 2012.
[20] O. Bulan *et al*., "Segmentation- and Annotation-Free License Plate Recognition With Deep Localization and Failure Identification," *IEEE Trans. on Intell. Transp. Syst.*, vol. 18, no. 9, pp. 2351-2363, Sep. 2017.
[21] X. Sun *et al.* , "A Generic Framework for Monitoring Local Freight Traffic Movements Using Computer Vision-based Techniques," *5th IEEE Intern. Conf. on Models and Technologies for Intell. Transp. Sys. (MT-ITS)*, pp. 63-68, 2017.
[22] R. A. Primerano, "High Bit-rate Digital Communication through Metal Channels," Ph.D. dissertation, Faculty of Drexel University, July 2010.
[23] R. Vaughan, N. Scott, and D. White, "The theory of bandpass sampling," *IEEE Trans. Signal Process.*, vol. 39, no. 9, pp. 1973–1984, Sep. 1991.
[24] J. R. G. Oya *et al*., "Design of Dual-Band Multi-Standard Subsampling Receivers for Optimal SNDR in Nonlinear and Interfering Environments," IEEE Trans. on Instr. Meas., vol. 63, no. 4, pp. 981-983, Apr. 2014.
[25] "Narrowband orthogonal frequency division multiplexing power line communication transceivers for PRIME networks", ITU-T Rec.9904, Oct. 2012.